Proceedings of the Czech–Japanese Seminar in Applied Mathematics 2006
Czech Technical University in Prague, September 14-17, 2006
pp. 177–184

NUMERICAL SOLUTION OF HIGHER AND LOWER MACH NUMBER FLOWS

KAREL KOZEL[1], PETRA PUNČOCHÁŘOVÁ[2], JIŘÍ FÜRST[2], AND JAROMÍR HORÁČEK[1]

Abstract. The work deals with numerical solution of two compressible flows problems. Firstly authors considered steady transonic flows through DCA 8% cascade (Double Circular Arc symmetrical) for increasing upstream Mach numbers $M_\infty \in (0.813; 1.13)$. The cascade flows were suggested in Institute of Thermomechanics by Mr. Dvořák and flows were investigated experimentally. The structure of flow seems to be very complicated. It is possible to observe subsonic and supersonic part, shock wave structure, interaction of shock wave and boundary layer, wake etc. We investigated these flows numerically using composite scheme in the form of finite volume method for governing system of Euler equations. These numerical results are compared to experimental data of IT CAS CZ using comparison of several regimes with increasing upstream Mach numbers.

The second problem is an unsteady viscous flow with very low upstream Mach number $M_\infty \approx 0.02$ in a 2D channel with a moving part of solid wall as a function of time. The flow is described by the system of Navier-Stokes equations for compressible laminar flows. The problem is numerically solved by MacCormack finite volume scheme. Moved grid of quadrilateral cells is considered in the form of conservation laws using Arbitrary Lagrangian-Eulerian method.

Key words. CFD, FVM, Euler equations, Navier-Stokes equations, composite Lax-Friedrichs and Lax-Wendroff scheme, MacCormack scheme, DCA cascade, moving grid.

AMS subject classifications. 35K60, 35K65, 65N06, 68U10

1. Introduction. This work presents a numerical solution of two compressible flows problems with higher and lower inlet Mach numbers. The first problem is a numerical solution of steady inviscid flow through cascade with double circular arc symmetrical 8% profiles (DCA 8%) and inlet Mach numbers $M_\infty \in (0.813; 1.13)$. The numerical solution of Euler equations is achieved by explicit central finite volume method using a composite scheme. The second problem presents unsteady numerical solution of the system of Navier-Stokes equations for compressible viscous laminar flow in a symmetrical channel. Unsteady flow is caused by a moving part of the channel wall as a function of time. Physically the flow in the symmetrical channel can present a very simple model of flow in a human vocal tract. Numerical solution is achieved by explicit predictor-corrector finite volume version of MacCormack scheme on a moved grid of quadrilateral cells.

2. Mathematical model. The 2D system of Navier-Stokes equations (2.1) has been used as mathematical model to describe an unsteady, viscous compressible (laminar) flow in a channel. The system is expressed in non-dimensional form:

$$W_t + F_x + G_y = \frac{1}{Re}(R_x + S_y), \tag{2.1}$$

$W = [\rho, \rho u, \rho v, e]^T$ is the vector of conservative variables, $F = [\rho u, \rho u^2 + p, \rho uv, (e+p)u]^T$ and $G = [\rho v, \rho uv, \rho v^2 + p, (e+p)v]^T$ are the vectors of inviscid fluxes, $R =$

[1]Institute of Thermomechanics, Czech Academy of Sciences, Centre of Energetics
[2]Czech Technical University in Prague, Faculty of Mechanical Engineering, Department of Technical Mathematics

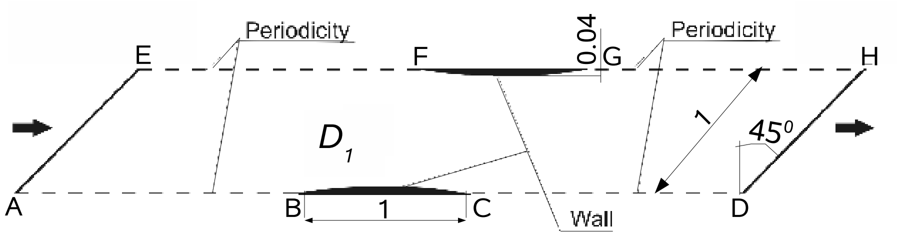

FIG. 3.1. *Domain of solution D_1 of DCA 8% cascade.*

$[0, \frac{2}{3}\eta(2u_x - v_y), \eta(u_y + v_x), uR_2 + vR_3 + kT_x]^T$ and $S = [0, \eta(u_y + v_x), \frac{2}{3}\eta(-u_x + 2v_y), uS_2 + vS_3 + kT_y]^T$ are the vectors of viscous fluxes. Reynolds number $Re = \frac{\rho_\infty u_\infty H}{\eta_\infty}$ is computed from inflow variables. Dynamic viscosity is $\eta = \frac{1}{Re}$ and temperature is $T = \frac{p}{r\rho}$. Static pressure p in the inviscid fluxes is expressed by the equation of state. If a flow is considered to be inviscid, Euler equations are used and then the right side of the equation (2.1) is equal to zero.

3. Inviscid steady compressible flow through DCA 8% cascade. For numerical solution the domain of solution D and its boundary conditions are defined. Figure 3.1 shows domain of solution D_1 which is one period of the DCA 8% cascade [1, 2]. The lower curve $\overset{\frown}{BC}$ and upper curve $\overset{\frown}{FG}$ represent solid wall and the parts $\overline{AB}$, $\overline{CD}$, $\overline{EF}$ and $\overline{GH}$ represent periodical boundaries. The inlet boundary is between points A, E and the outlet boundary is between points D, H. Boundary conditions are considered in the following form:

a) Upstream conditions: 3 values of W are given, pressure is extrapolated.
b) Downstream conditions: pressure is given, other values are extrapolated.
c) On the solid wall non-slip condition is considered $(u, v)_{wall} \cdot \vec{n} = 0$.
d) Periodicity condition for all variables.

3.1. Numerical solution of flow through DCA 8% cascade. Numerical solution of the system of Euler equations which describes inviscid compressible flow is realized by a composite finite volume scheme [3] on a grid of quadrilateral cells:

$$W_{i,j}^{n+1} = W_{i,j}^n - \frac{\Delta t}{\mu_{i,j}} \sum_{k=1}^{4} (\tilde{F}_k^n \Delta y_k - \tilde{G}_k^n \Delta x_k) + \frac{\epsilon}{4} \sum_{k=1}^{4} (W_k^n - W_{i,j}^n) \tag{3.1}$$

$$\begin{aligned} &\text{predictor step :} \\ &W_{i,j}^{n+1/2} = W_{i,j}^n - \frac{\Delta t}{2} \frac{1}{\mu_{i,j}} \sum_{k=1}^{4} (\tilde{F}_k^n \Delta y_k - \tilde{G}_k^n \Delta x_k) + \frac{\epsilon}{4} \sum_{k=1}^{4} (W_k^n - W_{i,j}^n) \\ &\text{corrector step :} \\ &W_{i,j}^{n+1} = W_{i,j}^n - \frac{\Delta t}{\mu_{i,j}} \sum_{k=1}^{4} (\tilde{F}_k^{n+1/2} \Delta y_k - \tilde{G}_k^{n+1/2} \Delta x_k) \end{aligned} \tag{3.2}$$

The Equation (3.1) is Lax-Friedrichs explicit scheme which is of the 1st order of accuracy in time and space and the Equation (3.2) is Lax-Wendroff explicit scheme in predictor-corrector form (Richtmyer form) which is of the 2^{nd} order of accuracy. The parameter $\mu_{i,j} = \int_{D_{i,j}} dxdy$ is volume of cell $D_{i,j}$ and parameter $\epsilon \in (0, 1)$. Numerical

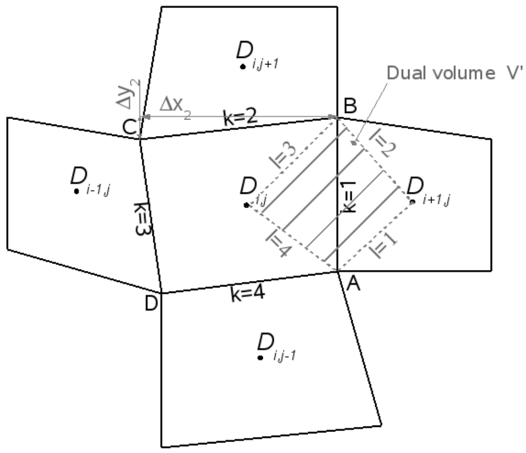

FIG. 3.2. *Finite volume $D_{i,j}$, dual volume V'_k.*

fluxes $\tilde{F}, \tilde{G}$ on edge k of cell $D_{i,j}$ (see Figure 3.2) are centrally approximated from physical fluxes F, G, e.g.: $\tilde{F}_1^n = \frac{1}{2}(F_{i,j}^n + F_{i+1,j}^n)$. The composite scheme ($CS$) is combined from Lax-Friedrichs (LF) scheme and from Lax-Wendroff (LW) scheme in the form:

$$CS = n \cdot LF + m \cdot LW \tag{3.3}$$

where $n = 1$ and m are numbers of time steps. Stability condition of the composite scheme (on regular orthogonal grid) reduces time step to:

$$\Delta t \leq \frac{CFL}{\frac{|u_{max}|+c}{\Delta x} + \frac{|v_{max}|+c}{\Delta y}}, \tag{3.4}$$

where c denotes local speed of sound and condition $CFL < 1$.

Remark 1: Composite scheme was originally published in [4] for finite difference scheme on orthogonal grid, extended in [3] for finite volume schemes for triangular and later for quadrilateral meshes. Number of iterations m in (3.3) depends on geometry, mesh etc. and has to be experimentally tested, because smoothing step by LF scheme has to be such small as possible.

3.2. Numerical results and comparison with experiment. The figures 3.3 and 3.4 show some transonic and supersonic flows for increasing upstream Mach numbers $M_\infty \in (0.813; 1.13)$ through DCA 8% cascade. Interferometric measurements of IT CAS CZ by Mr. Dvořák are shown on the left side in pictures. Numerical results computed by the composite scheme on structured mesh 150 x 30 cells are shown on the right side in pictures. The results are mapped by Mach number iso-lines ($\Delta M = 0.025$). Sonic line is marked by dashed line in the interferograms and by thick line in numerical results. We can compare change of upstream part of the flow using a change of sonic line as well as change downstream of the flow. Numerical results are similar to interferograms in upstream part of flow. Differences are observed between numerical and experimental data in downstream part because of inviscid flows considered in numerical results.

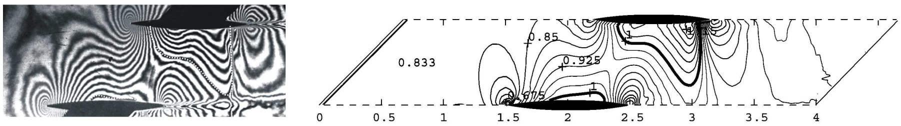

(a) Exp.: $M_\infty = 0.832$, $\alpha = 0^o$; Num.: $M_\infty = 0.850$, $\alpha = 0.9^o$, $m = 90$

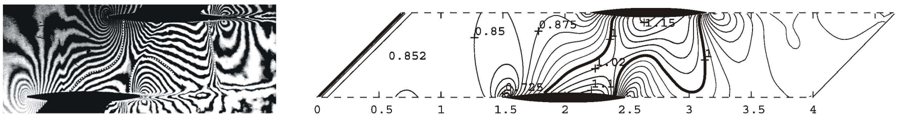

(b) Exp.: $M_\infty = 0.849$, $\alpha = 0^o$; Num.: $M_\infty = 0.930$, $\alpha = -2.0^o$, $m = 20$

FIG. 3.3. *Transonic flows. Comparison of experimental and numerical results.*

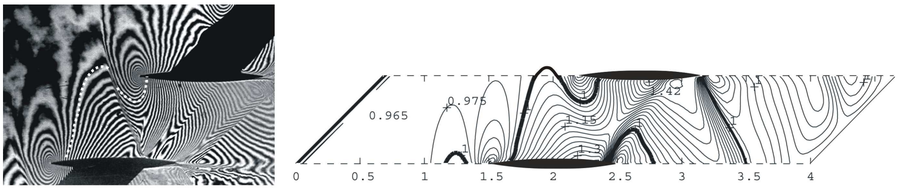

(a) Exp.: $M_\infty = 0.946$, $\alpha = 0^o$; Num.: $M_\infty = 1.050$, $\alpha = 0^o$, $m = 40$

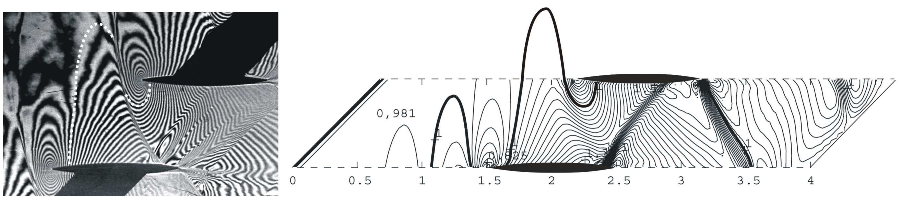

(b) Exp.: $M_\infty = 0.982$, $\alpha = 0^o$; Num.: $M_\infty = 1.080$, $\alpha = 0^o$, $m = 70$

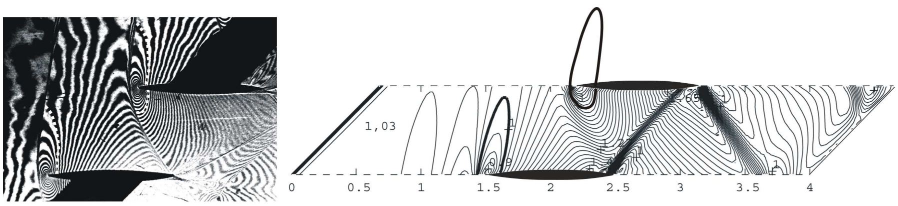

(c) Exp.: $M_\infty = 1.073$, $\alpha = 0^o$; Num.: $M_\infty = 1.150$, $\alpha = 0^o$, $m = 40$

FIG. 3.4. *Supersonic flows. Comparison of experimental and numerical results.*

4. Unsteady viscous compressible flow in symmetrical channel. Figure 4.1 shows domain of solution D_2 called the symmetrical channel. The computational domain is only the lower half of the channel. The upper boundary represents the axis of symmetry. Lower boundary represents solid wall and part of wall between points A, B is changing as a given function of time $g(t)$. Boundary conditions are considered in the following form:

a) Upstream conditions: 3 values of W are given, pressure is extrapolated.

b) Downstream conditions: pressure is given, other values are extrapolated.

c) On the solid wall velocity vector $(u, v)_{wall} = \vec{0}$ and temperature $T_n = 0$ are considered.

d) At the axis of symmetry $(u, v) \cdot \vec{n} = 0$ is considered.

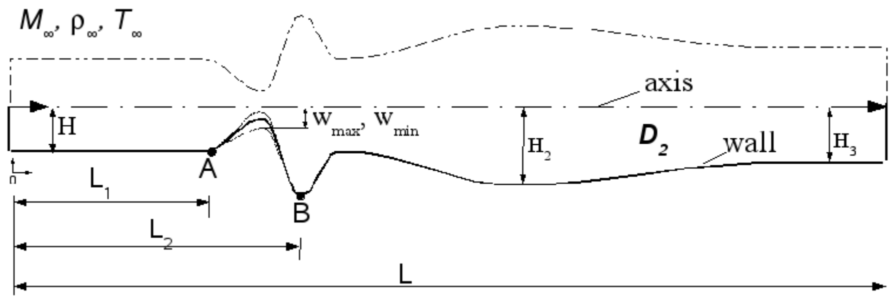

FIG. 4.1. *Domain of solution D_2 the symmetrical channel.*

4.1. Numerical solution of flow in a symmetrical channel. For numerical solution of the system (2.1) explicit MacCormack finite volume scheme in predictor corrector form which is of the 2nd order of accuracy in time and space is used.

$$W_{i,j}^{n+1/2} = \frac{\mu_{i,j}^n}{\mu_{i,j}^{n+1}} W_{i,j}^n - \frac{\Delta t}{\mu_{i,j}^{n+1}} \sum_{k=1}^{4} [(\tilde{F}_k^n - s_{1k} W_k^n - \tilde{R}_k^n)\Delta y_k - (\tilde{G}_k^n - s_{2k} W_k^n - \tilde{S}_k^n)\Delta x_k]$$

$$\overline{W}_{i,j}^{n+1} = \frac{\mu_{i,j}^n}{\mu_{i,j}^{n+1}} \frac{1}{2}(W_{i,j}^n + W_{i,j}^{n+1/2}) - \frac{\Delta t}{2\mu_{i,j}^{n+1}} \sum_{k=1}^{4} [(\tilde{F}_k^{n+1/2} - s_{1k} W_k^{n+1/2} - \tilde{R}_k^{n+1/2})\Delta y_k$$

$$-(\tilde{G}_k^{n+1/2} - s_{2k} W_k^{n+1/2} - \tilde{S}_k^{n+1/2})\Delta x_k] \tag{4.1}$$

Equation (4.1) represents MacCormack scheme for viscous flow in a domain with moving grid of quadrilateral cells. Moving grid in unsteady domain is described using Arbitrary Lagrangian-Eulerian (ALE) method which defines projection of reference domain D_0 to a domain in time D_t [5]. It defines other fluxes $\vec{s}_k W_k$ in MC scheme where vector $\vec{s}_k$ represents a velocity of edge k. Approximations of conservative variable W_k and diffusive components R_k, S_k on edge k are central. The second derivatives (dissipative terms) on edge are approximated using dual volumes [7] as is shown in Figure 3.2.

Inviscid numerical fluxes are approximated as follows:

$$\begin{aligned} &\tilde{F}_1^n = F_{i,j}^n, \tilde{F}_1^{n+1/2} = F_{i+1,j}^{n+1/2}, \tilde{F}_3^n = F_{i-1,j}^n, \tilde{F}_3^{n+1/2} = F_{i,j}^{n+1/2}, \\ &\tilde{G}_2^n = G_{i,j}^n, \tilde{G}_2^{n+1/2} = G_{i,j+1}^{n+1/2}, \tilde{G}_4^n = G_{i,j-1}^n, \tilde{G}_4^{n+1/2} = G_{i,j}^{n+1/2}, \text{etc.} \end{aligned} \tag{4.2}$$

The last term of MC scheme is Jameson artificial dissipation $AD(W_{i,j})^n$ that is added to schemes with higher order of accuracy to stabilise a numerical solution [6]:

$$AD(W_{i,j})^n = C_1\gamma_1(W_{i+1,j}^n - 2W_{i,j}^n + W_{i-1,j}^n) + C_2\gamma_2(W_{i,j+1}^n - 2W_{i,j}^n + W_{i,j-1}^n). \tag{4.3}$$

$C_1, C_2 \in R$ are constants and normed pressure gradients have form:

$$\gamma_1 = \frac{|p_{i+1,j}^n - 2p_{i,j}^n + p_{i-1,j}^n|}{|p_{i+1,j}^n| + 2|p_{i,j}^n| + |p_{i-1,j}^n|}, \gamma_2 = \frac{|p_{i,j+1}^n - 2p_{i,j}^n + p_{i,j-1}^n|}{|p_{i,j+1}^n| + 2|p_{i,j}^n| + |p_{i,j-1}^n|}. \tag{4.4}$$

Then we can compute a vector of conservative variables W in a new time level t^{n+1}:

$$W_{i,j}^{n+1} = \overline{W}_{i,j}^{n+1} + AD(W_{i,j})^n. \tag{4.5}$$

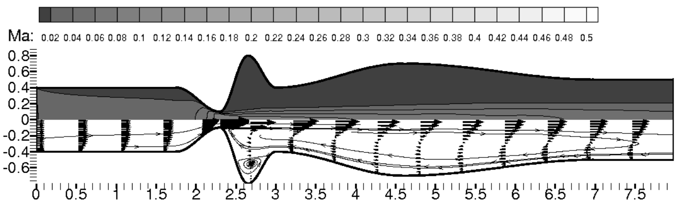

(a) Steady solution, initial state $t = 0$

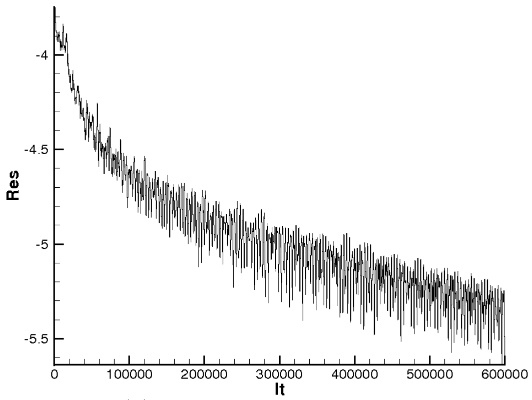

(b) Convergence to a steady solution

FIG. 4.2. *The steady numerical solution of viscous compressible (laminar) flow in the symmetrical channel,* $M_\infty = 0.02$*,* $Re \approx 9 \cdot 10^3$*,* $M_{max} = 0.0938$*, 400x50 cells.*

Stability condition of the MacCormack scheme (on regular orthogonal grid) reduces time step to:

$$\Delta t \leq \frac{CFL}{\frac{|u_{max}|+c}{\Delta x_{min}} + \frac{|v_{max}|+c}{\Delta y_{min}} + \frac{2}{Re}\left(\frac{1}{\Delta x^2_{min}} + \frac{1}{\Delta y^2_{min}}\right)}, \tag{4.6}$$

where c denotes local speed of sound, condition $CFL < 1$ and minimal step of grid in y-direction is $\Delta y_{min} \approx \frac{1}{\sqrt{Re}}$ due to boundary layer.

4.2. Numerical results of unsteady viscous flow in the channel. The domain D_2 contains 400x50 cells for length $L = 8$ and width of computed domain $H = 0.4$. Parameters considered for computation are set: inlet Mach number $M_\infty = 0.02$ (v_∞=6.68 m/s), dimension frequency of solid wall between points A, B (see Fig. 4.1) is $f = 20$ Hz and Reynolds number is $Re \approx 9 \cdot 10^3$. Figure 4.2(a) shows a steady solution of viscous laminar flow in the symmetrical channel. Maximal Mach number in domain was computed $M_{max} = 0.0938$. Figure 4.2(b) shows convergence to a steady solution that is followed using L_2 norm of momentum residuals (ρu). It seems to be relatively good for this case with very low Mach number. Figure 4.3 shows development of the unsteady viscous compressible laminar flows in the domain D_2 in several time layers in the third period of oscillations. For computation of the unsteady solution the steady solution was used as an initial state. The highest Mach number was achieved when the minimum gap was reached, nearly after the glottal-width began to open. The maximum computed value of Mach number is $M_{max} = 0.5174$ at the point $x = 2.325$ at the channel axis in time $t = 21/40\ \pi$. Domain D_2 with its boundary conditions represents a simple case of flow in a human vocal tract [8, 9].

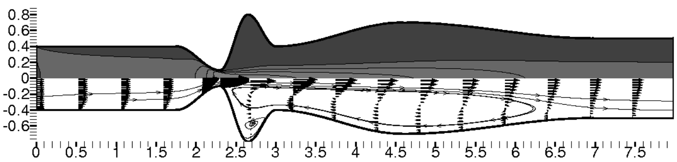

(a) $t = 4\pi, M_{max} = 0.0935$

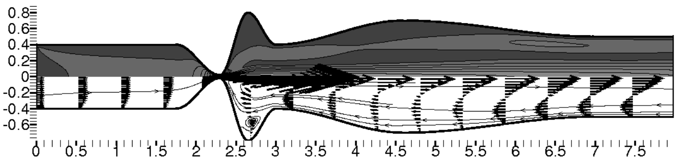

(b) $t = 4\pi + \frac{\pi}{2}, M_{max} = 0.5139$

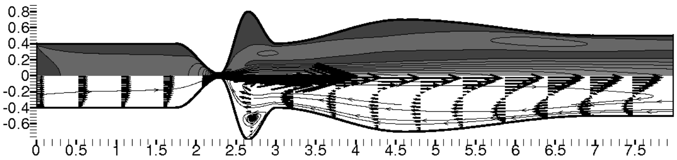

(c) $t = 4\pi + 21\pi/40, M_{max} = 0.5174$

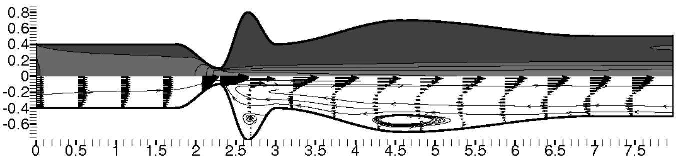

(d) $t = 5\pi, M_{max} = 0.0949$

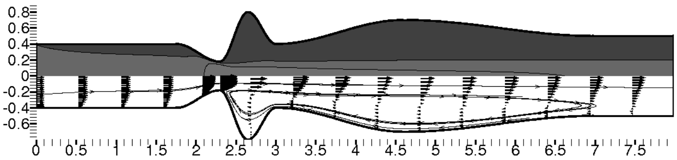

(e) $t = 4\pi + \frac{3\pi}{2}, M_{max} = 0.0523$

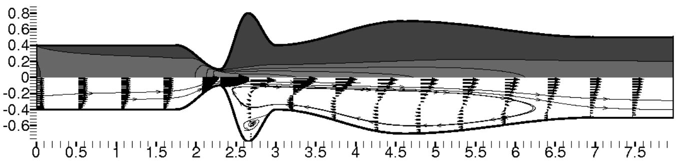

(f) $t = 6\pi, M_{max} = 0.0935$

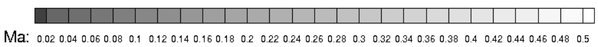

(g) Legend of Mach numbers

FIG. 4.3. *The unsteady numerical solution of viscous compressible (laminar) flow in the symmetrical channel, $M_\infty = 0.02$, $Re \approx 9 \cdot 10^3$, 400x50 cells.*

5. Conclusions. In the first case a numerical method solving 2D compressible system of Euler equations using finite volume method was developed. This method was realized for high Mach number flows in DCA 8% cascade. It was numerical simulation of CS scheme to show that also this scheme with accuracy of $k \in (1, 2)$ order is able to successfully simulate real high speed transonic flows. The numerical results were compared to interferometric measurements of IT CAS CZ. Comparison seems to be very good in upstream part of the flow-field and part between the profiles. The flow in downstream part shows some differences caused by the fact that real flow is viscous but for numerical solution only inviscid model has been used.

In the second case a numerical method solving 2D unsteady compressible system of Navier-Stokes equations using finite volume method was developed. This unsteady method was realized for very low Mach number flows in a 2D channel with changing part of solid wall as a given function of time. It is interesting, that in flows with very low Mach numbers described by the system of Euler equations is necessary to modify traditional numerical methods to converge in this problem but for the system of Navier-Stokes equations these methods are working well. For the case of vocal tract simulation by compressible viscous system, these unsteady results are one of the first in the world.

Acknowledgement. This work was supported by grant GA AV ČR No. IAA 2007 60613 and by Research Plan MSM No. 6840770010.

REFERENCES

[1] K. Kozel, J. Polášek, M. Vavřincová, Numerical education of transonic flow through a cascade with slender profiles. *Proceedings of the sixth international methods in fluid dynamics.* Tbilisi, 1978, Vol. 1, pp. 166–171.

[2] R. Dvořák, *Transsonické proudění.* Academia, Praha (1986).

[3] Janda, R., Kozel, K., Liska, R., Composite Scheme on Triangular Meshes. H. Freistühler, G. Warnecke (Eds.), *Hyperbolic Problems: Theory, Numerics, Applications, Vol. II* Birkhäuser Vortag - Berlin, 2002, pp. 563–572, ISBN 3-7643-6710-5.

[4] R. Liska, and B. Wendroff, *Composite Schemes for Conservation Laws*, SIAM J. Sci. Comput. **35**, no. 6 (1998), 2250–2271.

[5] R. Honzátko, K. Kozel, J. Horáček, Flow over a profile in a channel with dynamical effects. *Proceedings in Applied Mathematics and Mechanics.* Vol. 4, No. 1, 2004, pp. 322–323, ISSN 1617-7061.

[6] Jameson, A., Schmidt, W., Turkel, E., Numerical Solution of the Euler Equations by Finite Volume Methods Using Runge-Kutta Time-Stepping Schemes. AIAA, Paper 81-1250, 1981.

[7] J. Fürst, M. Janda, K. Kozel, Finite volume solution of 2D and 3D Euler and Navier-Stokes equations. J. Neustupa, P. Penel (Eds.), *Mathematical fluid mechanics.* Berlin, 2001, ISBN 3-7643-6593-5.

[8] P. Punčochářová, K. Kozel, J. Fürst, Unsteady, subsonic inviscid and viscous flows in a channel. *Fluid Dynamics 2005.* IT CAS CZ, 2005, pp. 125–128, ISBN 80-85918-94-3.

[9] J. Horáček, P. Šidlof, G. Švec, *Numerical simulation of self-oscillations of human vocal folds with Hertz model of impact forces.* Journal of Fluid and Structures **20** (2005), 853–869.